

FEM analysis and monolithic Newton-multigrid solver for thixo-viscoplastic flow problems

N. Begum, A. Ouazzi, S. Turek
Institute of Applied Mathematics, LS III,
TU Dortmund University, Dortmund, Germany

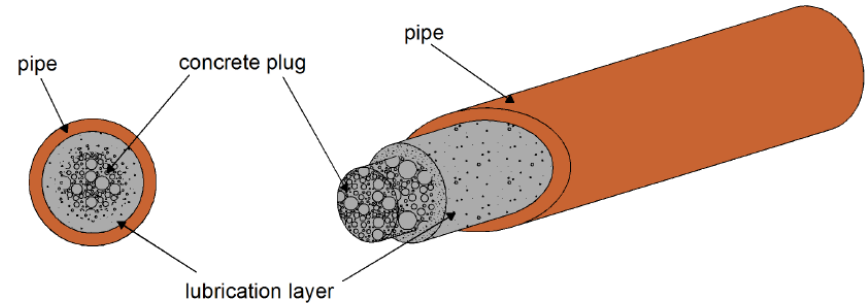
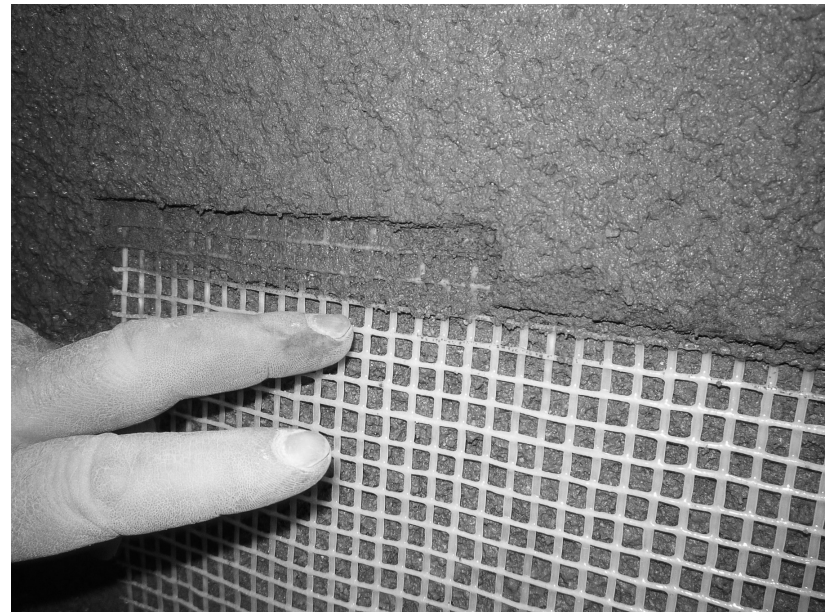
8th European Congress on Computational Methods in Applied Sciences and Engineering
ECCOMAS Congress 2022
5-9 June 2022, Oslo, Norway

Why “Thixotropic materials?

- Processing of thixotropic materials relevant for industrial applications
 - ➔ Lubrication, asphalt, self-compacting concrete...
- Physically fascinating due to improved mechanical properties

Goal:

- Modern CFD methods with high accuracy, robustness and efficiency for thixotropic materials
 - ➔ Saving time, money and resources



Investigation of solid/liquid and liquid/solid transitions based on micro-structure

- Thixotropy means
 - combination of two greek words
 - Thixis: shaking/stirring
 - trepo: turning/changing
- Thixotropy concept
 - Based on viscosity
 - Flow induced by time-dependent decrease of viscosity
 - The phenomena is reversible
- Rejuvenation / Breakdown
 - “Faster” flow: fluid rejuvenates
 - Decreases of viscosity with acceleration of the flow
- Aging / Buildup
 - At rest or under slow flow: fluid ages
 - Increases of the viscosity in time



HPC features:

- Moderately parallel
- GPU computing
- Open source



Hardware-oriented Numerics

Numerical features:

- Higher order **FEM** in space & (semi-) **Implicit** FD/FEM in time
- Semi-(un)structured meshes with dynamic **adaptive grid** deformation
- Fictitious Boundary (FBM) methods
- **Newton-Multigrid**-type solvers

Non-Newtonian flow module:

- generalized Newtonian model (Power-law, Carreau, Houska,...)
- viscoelastic differential model (Giesekus, FENE, Oldroyd,...)

Multiphase flow module (resolved interfaces):

- l/l – interface capturing (Level Set)
- s/l – interface tracking (FBM)
- s/l/l – combination of l/l and s/l

Engineering aspects:

- Geometrical design
- Modulation strategy
- Optimization

Here: FEM-based tools for the accurate simulation of (thixotropic) flow problems, particularly with complex rheology



For details, please visit: www.featflow.de

→ starting point: Generalized Navier-Stokes equations (+initial and boundary conditions)

$$\rho \left(\frac{\partial}{\partial t} + \mathbf{u} \cdot \nabla \right) \mathbf{u} - \nabla \cdot \boldsymbol{\sigma} + \nabla p = \rho f,$$
$$\nabla \cdot \mathbf{u} = 0,$$

- velocity- and pressure field \mathbf{u} and p
- stress tensor $\boldsymbol{\sigma}$
- linear material behaviour - Newtonian fluids

$$\boldsymbol{\sigma} = 2\eta_s \mathbf{D}(\mathbf{u}) \quad : \eta_s \text{ is constant viscosity}$$

- non-linear material behaviour- structurally viscous / viscoplastic

$$\boldsymbol{\sigma} = 2\eta_s(D_{\mathbb{II}}, p, \Theta, \lambda) \mathbf{D}(\mathbf{u}), \quad D_{\mathbb{II}} = \text{tr} \left(\frac{1}{2} \mathbf{D}(\mathbf{u})^2 \right)$$


- Power-law, Carreau, Bingham, Herschel-Bulkley, Houska, ...

- structure parameter λ

- Archetypical thixotropic viscoplastic (TVP) models

$$\begin{cases} \sigma = 2\eta(D_{\text{II}}, \lambda)\mathbf{D}(\mathbf{u}) + \sqrt{2}\tau(\lambda)\frac{\mathbf{D}(\mathbf{u})}{\sqrt{D_{\text{II}}}} & \text{if } D_{\text{II}} \neq 0 \\ \sigma_{\text{II}} \leq \tau(\lambda) & \text{if } D_{\text{II}} = 0 \end{cases}$$

- Relations between rheological parameters and structural parameter

	$\eta(D_{\text{II}}, \lambda)$	$\tau(\lambda)$
Worrall and Tulliani ¹	$\lambda\eta_0$	τ_0
Coussot <i>et al.</i> ²	$\lambda^a\eta_0$	—
Houska ³	$(\eta_0 + \eta_1\lambda)D_{\text{II}}^{\frac{(n-1)}{2}}$	$(\tau_0 + \tau_1\lambda)$
Mujumbar <i>et al.</i> ⁴	$(\eta_0 + \eta_1\lambda)D_{\text{II}}^{\frac{(n-1)}{2}}$	$\lambda^{a+1}G_0\Lambda_c^*$
Burgos <i>et al.</i> ⁵	η_0	$\lambda\tau_0$
Dullaert & Mewis ⁶	$\lambda\eta_0$	$\lambda G_0 \left(\lambda D_{\text{II}}^{\frac{1}{2}} \right) \Lambda_c^*$

* Λ_c is a constant/variable elastic strain.



- General format of evolution equation for structural parameter:

$$\frac{\partial \lambda}{\partial t} + u \cdot \nabla \lambda = F_{buildup} - F_{breakdown}$$

- Expressions for different thixotropic models:

	$F_{buildup}$	$F_{breakdown}$
Worrall and Tulliani ¹	$c_1(1 - \lambda)D_{II}^{\frac{1}{2}}$	$c_2\lambda D_{II}^{\frac{1}{2}}$
Coussot <i>et al.</i> ²	c_1	$c_2\lambda D_{II}^{\frac{1}{2}}$
Houska ³	$c_1(1 - \lambda)$	$c_2\lambda^m D_{II}^{\frac{1}{2}}$
Mujumbar <i>et al.</i> ⁴	$c_1(1 - \lambda)$	$c_2\lambda D_{II}^{\frac{1}{2}}$
Burgos <i>et al.</i> ⁵	$c_1(1 - \lambda)$	$c_2\lambda D_{II}^{\frac{1}{2}} \exp(aD_{II}^{\frac{1}{2}})$
Dullaert & Mewis ⁶	$(c_1 + c_3 D_{II}^{\frac{1}{2}})(1 - \lambda)t^{-b}$	$c_2\lambda D_{II}^{\frac{1}{2}}t^{-b}$

● Viscoplastic (VP) flow

$$\begin{cases} \boldsymbol{\sigma} = 2\eta_0 \mathbf{D}(\mathbf{u}) + \sqrt{2}\tau_0 \frac{\mathbf{D}(\mathbf{u})}{\sqrt{D_{\text{II}}}} & \text{if } D_{\text{II}} \neq 0 \\ \sigma_{\text{II}} \leq \tau_0 & \text{if } D_{\text{II}} = 0 \end{cases}$$

● Thixo-viscoplastic (TVP) flow

$$\begin{cases} \boldsymbol{\sigma} = 2\eta(D_{\text{II}}, \lambda) \mathbf{D}(\mathbf{u}) + \sqrt{2}\tau(\lambda) \frac{\mathbf{D}(\mathbf{u})}{\sqrt{D_{\text{II}}}} & \text{if } D_{\text{II}} \neq 0 \\ \sigma_{\text{II}} \leq \tau(\lambda) & \text{if } D_{\text{II}} = 0 \end{cases}$$

● Micro-structure equation

$$\left(\frac{\partial}{\partial t} + \mathbf{u} \cdot \nabla \right) \lambda + \mathcal{M}(D_{\text{II}}, \lambda) = f_{\lambda}$$

$$\mathcal{M} := \mathcal{G} - \mathcal{F}$$



➤ Viscosity model for TVP flow

● Classical approximations

$$\begin{cases} I. & \frac{1}{\sqrt{D_{\mathbb{II},r}}} := \frac{1}{\sqrt{(D_{\mathbb{II}} + (k^{-1})^2)}} \\ II. & \frac{1}{\sqrt{D_{\mathbb{II},r}}} := \frac{1}{\sqrt{D_{\mathbb{II}}}} \left(1 - e^{-k\sqrt{D_{\mathbb{II}}}}\right) \end{cases}$$

● Extended viscosity defined on all domain

$$\mu(D_{\mathbb{II},r}, \lambda) = \eta(D_{\mathbb{II}}, \lambda) + \tau(D_{\mathbb{II}}, \lambda) \frac{\sqrt{2}}{2} \frac{1}{\sqrt{D_{\mathbb{II},r}}}$$

➤ Full set of equations

$$\begin{cases} \left(\frac{\partial}{\partial t} + \mathbf{u} \cdot \nabla \right) \mathbf{u} - \nabla \cdot \left(2\mu(D_{\mathbb{II},r}, \lambda) \mathbf{D}(\mathbf{u}) \right) + \nabla p = \mathbf{f}_u & \text{in } \Omega \\ \nabla \cdot \mathbf{u} = 0 & \text{in } \Omega \\ \left(\frac{\partial}{\partial t} + \mathbf{u} \cdot \nabla \right) \lambda + \mathcal{M}(D_{\mathbb{II}}, \lambda) = f_\lambda & \text{in } \Omega \end{cases}$$



► Sobolev spaces and notations

- $H^0(\Omega) := L^2(\Omega) = \left\{ v \mid \int_{\Omega} |v|^2 d\Omega < \infty \right\}$
- $L_0^2(\Omega) = \left\{ v \in L^2(\Omega) \mid \int_{\Omega} v d\Omega = 0 \right\}, \quad \|v\|_{0,\Omega} = \left(\int_{\Omega} |v|^2 d\Omega \right)^{\frac{1}{2}}$
- $H^1(\Omega) = \left\{ v \in L^2(\Omega) \mid \nabla v \in L^2(\Omega) \right\}, \quad \|v\|_{1,\Omega} = (\|v\|_{0,\Omega}^2 + \|\nabla v\|_{0,\Omega}^2)^{\frac{1}{2}}$
- $H_{\Gamma}^1(\Omega) = \left\{ v \in H^1(\Omega) \mid v|_{\Gamma} = 0, \Gamma \subset \partial\Omega \right\}$
- $H_0^1(\Omega) = \left\{ v \in H^1(\Omega) \mid v|_{\partial\Omega} = 0 \right\}$
- $H(\mathbf{u}, \Omega) = \left\{ v \in L^2(\Omega), \mathbf{u} \cdot \nabla v \in L^2(\Omega) \right\}, \quad \|v\|_{1,\mathbf{u}} = (\|v\|_{0,\Omega}^2 + \|\mathbf{u} \cdot \nabla v\|_{0,\Omega}^2)^{\frac{1}{2}}$

$$\Gamma^- = \{x \in \Gamma \subset \partial\Omega \mid \mathbf{u} \cdot \mathbf{n} < 0\}, \quad \Gamma^+ = \{x \in \Gamma \subset \partial\Omega \mid \mathbf{u} \cdot \mathbf{n} > 0\}$$

$$\langle v, w \rangle_{\pm} = \int_{\Gamma^{\pm}} |\mathbf{u} \cdot \mathbf{n}| v w ds, \quad \langle v \rangle_{\pm} = \langle v, v \rangle_{\pm}^{\frac{1}{2}}$$



- **Flow variables** (λ, \mathbf{u}, p)

- **Set** $\mathbb{T} := H_{\Gamma^-}^1(\Omega), \mathbb{V} := [H_0^1(\Omega)]^2, \mathbb{Q} := L^2(\Omega), \mathbb{W} := \mathbb{T} \times \mathbb{V}$
- **Set** $\tilde{\mathbf{u}} := (\lambda, \mathbf{u})$
- **Find** $(\lambda, \mathbf{u}, p) \in \mathbb{T} \times \mathbb{V} \times \mathbb{Q}$ **s.t.**

$$\langle \mathcal{K}(\lambda, \mathbf{u}, p), (\xi, \mathbf{v}, q) \rangle = \langle \mathcal{L}, (\xi, \mathbf{v}, q) \rangle, \quad \forall (\xi, \mathbf{v}, q) \in \mathbb{T} \times \mathbb{V} \times \mathbb{Q}$$

$$\mathcal{K} = \begin{bmatrix} \mathcal{A}_{\tilde{\mathbf{u}}} & \mathcal{B}^T \\ \mathcal{B} & 0 \end{bmatrix}$$

- **Compatibility constraints**

$$\sup_{\mathbf{v} \in \mathbb{V}} \frac{\langle \mathcal{B}\mathbf{v}, q \rangle}{\|\mathbf{v}\|_{\mathbb{V}}} \geq \beta \|q\|_{\mathbb{Q}/Ker \mathcal{B}^T}, \quad \forall q \in \mathbb{Q}$$



➤ Weak Formulation

$$\left\langle \mathcal{K}(\lambda, \mathbf{u}, p), (\xi, \mathbf{v}, q) \right\rangle = \left\langle \mathcal{L}, (\xi, \mathbf{v}, q) \right\rangle, \quad \forall (\xi, \mathbf{v}, q) \in \mathbb{T} \times \mathbb{V} \times \mathbb{Q}$$

➤ Operators

$$\left\langle \mathcal{K}(\lambda, \mathbf{u}, p), (\xi, \mathbf{v}, q) \right\rangle = a_\lambda(\tilde{\mathbf{u}})(\lambda, \xi) + a_{\mathbf{u}}(\tilde{\mathbf{u}})(\mathbf{u}, \mathbf{v}) + b(\mathbf{v}, p) - b(\mathbf{u}, q)$$

$$\mathcal{A}_{\tilde{\mathbf{u}}}(\tilde{\mathbf{u}})\tilde{\mathbf{u}} = \mathcal{A}_\lambda(\tilde{\mathbf{u}})\lambda + \mathcal{A}_{\mathbf{u}}(\tilde{\mathbf{u}})\mathbf{u}$$

$$\left\langle \mathcal{A}_\lambda(\tilde{\mathbf{u}})\lambda, \xi \right\rangle = a_\lambda(\tilde{\mathbf{u}})(\lambda, \xi) = \left(\mathcal{M}(D_{\mathbb{I}}, \lambda), \xi \right) + \left(\mathbf{u} \cdot \nabla \lambda, \xi \right)$$

$$\left\langle \mathcal{A}_{\mathbf{u}}(\tilde{\mathbf{u}})\mathbf{u}, \mathbf{v} \right\rangle = a_{\mathbf{u}}(\tilde{\mathbf{u}})(\mathbf{u}, \mathbf{v}) = \left(2\mu(D_{\mathbb{I},r}, \lambda) \mathbf{D}(\mathbf{u}), \mathbf{D}(\mathbf{v}) \right) + \left(\mathbf{u} \cdot \nabla \mathbf{u}, \mathbf{v} \right)$$

$$\left\langle \mathcal{B}\mathbf{v}, q \right\rangle = b(\mathbf{v}, q) = -\left(\nabla \cdot \mathbf{v}, q \right)$$

$$\left\langle \mathcal{L}, (\xi, \mathbf{u}, q) \right\rangle = \left(f_\lambda, \xi \right) + \left(\mathbf{f}_{\mathbf{u}}, \mathbf{v} \right)$$

Wellposedness of thixo-viscoplastic problem !



➤ Coerciveness

- ⦿ $a_\lambda(\tilde{\mathbf{v}})(\xi, \xi) \geq \alpha_0 \|\xi\|_{0,\Omega}^2 + \frac{1}{2} \left\{ \langle \xi \rangle_+^2 + \langle \xi \rangle_-^2 \right\} \quad \forall \xi \in \mathbb{T}$
- ⦿ $a_{\mathbf{u}}(\tilde{\mathbf{v}})(\mathbf{v}, \mathbf{v}) \geq \alpha_1 \|\mathbf{v}\|_{1,\Omega}^2 \quad \forall \mathbf{v} \in \mathbb{V}$

➤ Continuity

- ⦿ $a_\lambda(\tilde{\mathbf{u}})(\lambda, \xi) \leq |\mathbf{u}|_{0,\infty} \|\lambda\|_{0,\Omega} \|\xi\|_{1,\Omega} + K_1 \|\lambda\|_{0,\Omega} \|\xi\|_{0,\Omega} + \langle \lambda, \xi \rangle_+ \quad \forall \lambda, \xi \in \mathbb{T}$
 $\leq C_0 \|\lambda\|_{1,\Omega} \|\xi\|_{1,\Omega} \quad \forall \lambda, \xi \in \mathbb{T}$
- ⦿ $a_{\mathbf{u}}(\tilde{\mathbf{u}})(\mathbf{u}, \mathbf{v}) \leq (\mu_T + \tau_T) \|\mathbf{u}\|_{1,\Omega} \|\mathbf{v}\|_{1,\Omega} \quad \forall \mathbf{u}, \mathbf{v} \in \mathbb{V}$
 $\leq C_1 \|\mathbf{u}\|_{1,\Omega} \|\mathbf{v}\|_{1,\Omega} \quad \forall \mathbf{u}, \mathbf{v} \in \mathbb{V}$

Coercivity in weaker norm for the microstructure !



➤ Monotonicity

- $a_{\lambda}(\tilde{\boldsymbol{u}})(\lambda, \lambda - \xi) - a_{\lambda}(\tilde{\boldsymbol{v}})(\xi, \lambda - \xi) \geq \left(\mathcal{M}(D_{\text{II}}(\boldsymbol{u}), \lambda) - \mathcal{M}(D_{\text{II}}(\boldsymbol{v}), \xi), \lambda - \xi \right)$
 $\geq \alpha_0 \|\lambda - \xi\|_{0,\Omega} \quad \forall \lambda, \xi \in \mathbb{T}$

- $a_{\boldsymbol{u}}(\tilde{\boldsymbol{u}})(\boldsymbol{u}, \boldsymbol{u} - \boldsymbol{v}) - a_{\boldsymbol{v}}(\tilde{\boldsymbol{v}})(\boldsymbol{v}, \boldsymbol{u} - \boldsymbol{v}) \geq \mu_{\text{T}} |\boldsymbol{D}(\boldsymbol{u}) - \boldsymbol{D}(\boldsymbol{v})|^2$
 $+ \frac{\sqrt{2}}{2} \frac{\tau_{\text{T}}}{\sqrt{D_{\text{II},r}}} \left\{ \underbrace{|\boldsymbol{D}(\boldsymbol{u}) - \boldsymbol{D}(\boldsymbol{v})|^2}_{\text{I}} - \underbrace{\frac{\sqrt{2}}{2} \frac{|\boldsymbol{D}(\boldsymbol{u}) - \boldsymbol{D}(\boldsymbol{v})|}{\sqrt{D_{\text{II},r}}} (\boldsymbol{D}(\boldsymbol{v}), \boldsymbol{D}(\boldsymbol{u}) - \boldsymbol{D}(\boldsymbol{v}))}_{\text{II}} \right\}$
 $\geq \alpha_1 \|\boldsymbol{u} - \boldsymbol{v}\|_{1,\Omega} \quad (\text{I} \geq \text{II}) \quad \forall \boldsymbol{u}, \boldsymbol{v} \in \mathbb{V}$

Thixoviscoplastic problem has a unique solution



- **Conforming approximations**

$$\mathbb{T}_h \subset \mathbb{T}, \quad \mathbb{V}_h \subset \mathbb{V}, \quad \mathbb{Q}_h \subset \mathbb{Q}, \quad \mathbb{W}_h := \mathbb{T}_h \times \mathbb{V}_h$$

$$\mathcal{A}_{\tilde{\mathbf{u}}_h} = \mathcal{A}_{\tilde{\mathbf{u}}}, \quad \mathcal{B}_h = \mathcal{B}$$

- **Discrete inf-sup condition**

$$\sup_{\mathbf{v}_h \in \mathbb{V}_h} \frac{\langle \mathcal{B}_h \mathbf{v}_h, q_h \rangle}{\|\mathbf{v}_h\|_{\mathbb{V}}} \geq \beta_h \|q_h\|_{\mathbb{Q}/Ker \mathcal{B}_h^T}, \quad \forall q_h \in \mathbb{Q}_h$$

➤ **Find** $(\lambda_h, \mathbf{u}_h, p_h) \in \mathbb{T}_h \times \mathbb{V}_h \times \mathbb{Q}_h$ **s.t**

$$\left\langle \mathcal{K}(\lambda_h, \mathbf{u}_h, p_h), (\xi_h, \mathbf{v}_h, q_h) \right\rangle = \left\langle \mathcal{L}, (\xi_h, \mathbf{v}_h, q_h) \right\rangle, \quad \forall (\xi_h, \mathbf{v}_h, q_h) \in \mathbb{T}_h \times \mathbb{V}_h \times \mathbb{Q}_h$$

Order of convergence !



➤ **Coercivity in a weaker norm for microstructure**

$$\frac{\alpha_0}{2} \|\lambda - \lambda_h\|_{0,\Omega}^2 + \frac{1}{4} \langle \lambda - \lambda_h \rangle^2 \leq \frac{1}{\alpha_0} (1 + K_1 + |\mathbf{u}|_{0,\infty}) \inf_{\xi_h \in \mathbb{T}_h} \|\lambda - \xi_h\|_{1,\Omega}^2$$

$$\|\lambda - \lambda_h\|_{0,\Omega} \equiv h^r |\lambda|_{r+1,\Omega}$$

➤ **Regularization of TVP model**

$$\begin{aligned} \|\mathbf{D}(\mathbf{u}) - \mathbf{D}(\mathbf{u}_h)\|_{0,\Omega} &\leq \sqrt{2} \mu_{\text{T}}^{-1} \inf_{q_h \in \mathbb{Q}_h} \|p - q_h\|_{0,\Omega} \\ &\quad + (3 + 3\tau_{\text{T}}^2 \mathbf{k}^2 \mu_{\text{T}}^{-2})^{1/2} \inf_{\mathbf{v} \in \mathbb{V}_h} \|\mathbf{D}(\mathbf{u}) - \mathbf{D}(\mathbf{v}_h)\|_{0,\Omega} \end{aligned}$$

$$\begin{aligned} \|\mathbf{D}(\mathbf{u}) - \mathbf{D}(\mathbf{u}_h)\|_{0,\Omega} &\leq \sqrt{2} \mu_{\text{T}}^{-1} \inf_{q_h \in \mathbb{Q}_h} \|p - q_h\|_{0,\Omega} \\ &\quad + \sqrt{2} \inf_{\mathbf{v} \in \mathbb{V}_h} \|\mathbf{D}(\mathbf{u}) - \mathbf{D}(\mathbf{v}_h)\|_{0,\Omega} \\ &\quad + (2\tau_{\text{T}} \mu_{\text{T}}^{-1})^{1/2} \inf_{\mathbf{v} \in \mathbb{V}_h} \|\mathbf{D}(\mathbf{u}) - \mathbf{D}(\mathbf{v}_h)\|_{0,\Omega}^{\frac{1}{2}} \end{aligned}$$

Coercivity in a stronger norm for the microstructure eq. !

FEM choices to counterbalance the regularisation/sub-optimality !



- Discretization of TVP model have to address the following challenges
 - Stable FEM spaces
 - Coercivity in a weaker norm
 - Regularization
 - Convection domination
 - Monotonicity preserving and satisfying strongly DMP
- TVP Newton-multigrid Solver have to deal with
 - Different source of nonlinearities
 - Strong coupling of equations
 - Robustness and efficiency

✓ **The family of conforming FEM** $Q_r/Q_r/P_{r-1}^{\text{disc}}$, $r \geq 2$ **for** (λ, \mathbf{u}, p) **with stabilization**

- **Inf-sup conditions is satisfied**
- **Discontinuous pressure**
 - **Practical w.r.t. monolithic approach**
 - **Element-wise mass conservation**

✓ **Highly consistent and symmetric stabilization**

$$j_\lambda(\lambda_h, \xi_h) = \sum_{e \in \mathcal{E}_h} h^2 \gamma_\lambda \int_e [\nabla \lambda_h] : [\nabla \xi_h] d\Omega, \quad j_{\lambda,l} := j_\lambda \text{ for } \gamma_\lambda = \text{cst.}$$

$$j_{\mathbf{u}}(\mathbf{u}_h, \mathbf{v}_h) = \sum_{e \in \mathcal{E}_h} h^2 \gamma_{\mathbf{u}} \int_e [\nabla \mathbf{u}_h] : [\nabla \mathbf{v}_h] d\Omega, \quad j_{\mathbf{u},l} := j_{\mathbf{u}} \text{ for } \gamma_{\mathbf{u}} = \text{cst.}$$

- **Coercivity in a strong norm for the microstructure eq.**
- **Monotonocity preserving and satisfying strong DMP**
- **Efficient and robust w.r.t. multigrid solver**



➤ **Coercivity in a Stronger norm for microstructure**

$$\begin{aligned} |\!|\!|\lambda|\!|\!| &= \left(\alpha_0 |\!|\!|\lambda|\!|\!|_{0,\Omega} + \frac{1}{2} \langle \lambda \rangle^2 + j_{\lambda,l}(\lambda, \lambda) \right)^{\frac{1}{2}} \\ |\!|\!|\lambda - \lambda_h|\!|\!|^2 &\leq \frac{1}{\alpha_0} (1 + K_1 + |\boldsymbol{u}|_{0,\infty}) \inf_{\xi_h \in \mathbb{T}_h} \|\lambda - \xi_h\|_{1,\Omega}^2 \\ &\quad + \frac{1}{2} \inf_{\xi_h \in \mathbb{T}_h} j_{\lambda,l}(\lambda_h - \xi_h, \lambda_h - \xi_h) \\ \|\lambda - \lambda_h\|_{0,\Omega} &\equiv h^{r+\frac{1}{2}} |\lambda|_{r+1,\Omega} \end{aligned}$$

➤ **Regularisation for TVP model**

$$|\boldsymbol{u} - \boldsymbol{u}_h|_{1,\Omega} \equiv \sqrt{2} \mu_{\text{T}}^{-1} \mathcal{O}(h^r) + (3 + 3\tau_{\text{T}}^2 \mu_{\text{T}}^{-2})^{1/2} \mathcal{O}(\textcolor{red}{k} h^r)$$

$$|\boldsymbol{u} - \boldsymbol{u}_h|_{1,\Omega} \equiv \sqrt{2} \mu_{\text{T}}^{-1} \mathcal{O}(h^r) + \sqrt{2} \mathcal{O}(h^r) + (2\tau_{\text{T}} \mu_{\text{T}}^{-1})^{1/2} \mathcal{O}(h^{\frac{r}{2}})$$

$$|\boldsymbol{u} - \boldsymbol{u}_h|_{1,\Omega} \equiv \mathcal{O}(k^{-1}) \implies h \leq \mathcal{O}(k^{-\frac{2}{r}})$$

Stabilization recover the optimal order of convergence
Higher order FEM counterbalance regularization



Let $\{\varphi_i, i = 1, 2, \dots, \dim \mathbb{W}_h\}$ and $\{\psi_i, i = 1, \dots, \dim \mathbb{Q}_h\}$ denote the basis of spaces \mathbb{W}_h and \mathbb{Q}_h , respectively. The Solution $\mathcal{U} = (\lambda, \mathbf{u}, p) = (\tilde{\mathbf{u}}, p) \in \mathbb{W}_h \times \mathbb{Q}_h$

$$\mathcal{U} = \sum_{i=1}^{\dim \mathbb{W}_h} \tilde{\mathbf{u}}_i \varphi_i + \sum_{i=1}^{\dim \mathbb{Q}_h} p_i \psi_i$$

The residuals of discrete TVP problem $\mathcal{R}(\mathcal{U}) \in \mathbb{R}^{\dim \mathbb{W}_h + \dim \mathbb{Q}_h}$

$$\mathcal{R}(\mathcal{U}) = (\mathcal{R}_\lambda(\lambda, \mathbf{u}), \mathcal{R}_{\mathbf{u}}(\lambda, \mathbf{u}, p), \mathcal{R}_p(p)) = (\mathcal{R}_{\tilde{\mathbf{u}}}(\tilde{\mathbf{u}}, p), \mathcal{R}_p(p))$$

➤ Update of the nonlinear iteration with the correction $\delta \mathcal{U}$

$$\mathcal{U}^{l+1} = \mathcal{U}^l + \delta \mathcal{U}$$

➤ The linearization of the residual provides

$$\mathcal{R}(\mathcal{U}^{l+1}) = \mathcal{R}(\mathcal{U}^l + \delta \mathcal{U}) \simeq \mathcal{R}(\mathcal{U}^l) + \left(\frac{\partial \mathcal{R}(\mathcal{U}^l)}{\partial \mathcal{U}} \right) \delta \mathcal{U}$$

➤ The Newton's method assuming invertible Jacobian

$$\mathcal{U}^{l+1} = \mathcal{U}^l - \omega_l \left(\frac{\partial \mathcal{R}(\mathcal{U}^l)}{\partial \mathcal{U}} \right)^{-1} \mathcal{R}(\mathcal{U}^l)$$



The Jacobian matrix in discrete Newton is calculated using the finite difference

$$\left[\frac{\partial \mathcal{R}(\mathcal{U}^l)}{\partial \mathcal{U}} \right]_{ij} \approx \frac{\mathcal{R}_i(\mathcal{U}^l + \varepsilon_l e_j) - \mathcal{R}_i(\mathcal{U}^l - \varepsilon_l e_j)}{2\varepsilon_l}$$

➤ Damping of the updated solution, $\omega_l \in (0, 1)$, s.t.

$$\|\mathcal{R}(\mathcal{U}^{l+1})\| \leq \|\mathcal{R}(\mathcal{U}^l)\|$$

! Not sufficient for TVP problem

➤ Operator-adaptive splitting

$$\left(\frac{\partial \mathcal{R}(\mathcal{U}^l)}{\partial \mathcal{U}} \right) = \left(\frac{\partial \tilde{\mathcal{R}}(\mathcal{U})}{\partial \mathcal{U}} \right) + \delta_l \left(\frac{\partial \hat{\mathcal{R}}(\mathcal{U})}{\partial \mathcal{U}} \right)$$

$$\delta_{l+1} = f(r_l)\delta_l, \quad r_l := \|\mathcal{R}(\mathcal{U}^l)\|/\|\mathcal{R}(\mathcal{U}^{l-1})\|, \quad f(r_l) = 0.2 + 4/(0.7 + e^{1.5r_l})$$

! Requires a priori analysis of the Jacobian

➤ Adaptive step-length control

$$\varepsilon_{l+1} = g(r_l)\varepsilon_l, \quad g(r_l) = 1/f(r_l)$$

! Robust

Convergence analysis of the method !



The discretization and linearization of TVP leads to systems of following linearized discrete TVP saddle point problem

$$\left(\frac{\partial \mathcal{R}(\mathcal{U})}{\partial \mathcal{U}} \right) \delta \mathcal{U} = \begin{pmatrix} \frac{\partial \mathcal{R}_{\tilde{\mathbf{u}}}(\tilde{\mathbf{u}})}{\partial \tilde{\mathbf{u}}} & \frac{\partial \mathcal{R}_{\tilde{\mathbf{u}}}(\tilde{\mathbf{u}})}{\partial p} \\ \frac{\partial \mathcal{R}_p(\tilde{\mathbf{u}})}{\partial \tilde{\mathbf{u}}} & 0 \end{pmatrix} \begin{pmatrix} \delta \tilde{\mathbf{u}} \\ \delta p \end{pmatrix} = - \begin{pmatrix} \mathcal{R}_{\tilde{\mathbf{u}}} \\ \mathcal{R}_p \end{pmatrix}.$$

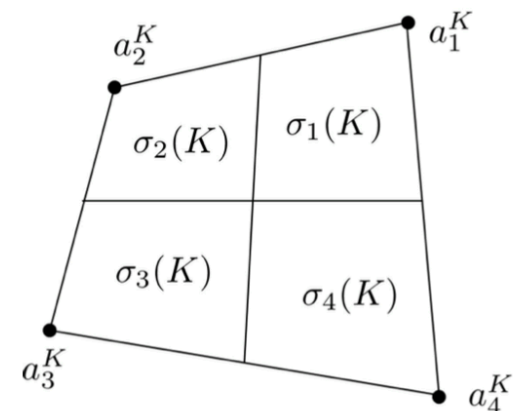
➤ Coupled geometric multigrid methods CGMG

- Hierarchy of multilevel triangulations
- Relaxation/smoothing
- Coarse-grid correction
- Grid transfer operator
- Local Multilevel Pressure Schur Complement

Linearized discrete TVP Saddle-point problem $\mathcal{J}\delta\mathcal{U} = \mathcal{R}$

- $\{\mathcal{T}_{h_k}\}$ denote a family of hierarchy of multi-level triangulation with step-size h_k
- Each element on triangulation $\mathcal{T}_{h_{k-1}}$ is splitted into $2^d, (d=2)$ new elements $\sigma_i(K), i = 1, \dots, 2^d$ to get \mathcal{T}_{h_k}
- The k^{th} level iteration $MG(k, \delta\mathcal{U}_0, \mathcal{R})$ of MG to solve

$$\mathcal{J}_k \delta\mathcal{U} = \mathcal{R}$$



◆ For $k = 1$ using the direct solver $MG(1, \delta\mathcal{U}_0, \mathcal{R}) = \mathcal{J}_1^{-1} \mathcal{R}$

◆ For $k > 1$

► Pre-smoothing step: $\delta\mathcal{U}_l = \delta\mathcal{U}_{l-1} + \mathcal{C}_k^{-1} (\mathcal{R} - \mathcal{J}_k \delta\mathcal{U}_{l-1}), 1 \leq l \leq \nu_1$

► Correction step: Let $\tilde{\mathcal{R}} = \mathcal{I}_k^{k-1} (\mathcal{R} - \mathcal{J}_k \delta\mathcal{U}_{\nu_1}), \mathcal{Z}_i \in \mathcal{V}_{k-1}, 0 \leq i \leq 2,$

$$\mathcal{Z}_0 = 0$$

$$\mathcal{Z}_1 = MG_F(k-1, \mathcal{Z}_0, \tilde{\mathcal{R}})$$

$$\mathcal{Z}_2 = MG_V(k-1, \mathcal{Z}_1, \tilde{\mathcal{R}})$$

► Final output: $MG(k, \delta\mathcal{U}_0, \mathcal{R}) = \delta\mathcal{U}_{\nu_1} + \mathcal{I}_{k-1}^k \mathcal{Z}_2$

► Post-smoothing step: $\delta\mathcal{U}_l = \delta\mathcal{U}_{l-1} + \mathcal{C}_k^{-1} (\mathcal{R} - \mathcal{J}_k \delta\mathcal{U}_{l-1}), 1 \leq l \leq \nu_2$

Geometric transfer between FE spaces

- **The coarse-to-fine grid (prolongation):** $\mathcal{I}_{k-1}^k = (\mathcal{I}_{k-1,k}^{\tilde{\mathbf{u}}}, \mathcal{I}_{k-1,k}^p)$
- **The fine-to coarse grid (restriction):** $\mathcal{I}_k^{k-1} = (\mathcal{I}_{k,k-1}^{\tilde{\mathbf{u}}}, \mathcal{I}_{k,k-1}^p)$

$$\begin{aligned}\mathcal{I}_{k,k-1}^{\tilde{\mathbf{u}}} : \mathbb{W}_{h_k} &\longrightarrow \mathbb{W}_{h_{k-1}}, & \mathcal{I}_{k-1,k}^{\tilde{\mathbf{u}}} : \mathbb{W}_{h_{k-1}} &\longrightarrow \mathbb{W}_{h_k}, \\ \mathcal{I}_{k,k-1}^p : \mathbb{Q}_{h_k} &\longrightarrow \mathbb{Q}_{h_{k-1}}, & \mathcal{I}_{k-1,k}^p : \mathbb{Q}_{h_{k-1}} &\longrightarrow \mathbb{Q}_{h_k}.\end{aligned}$$

- **Structure and velocity, Q_2 FEM approximations:**

Nested approximation , $\mathbb{W}_{h_{k-1}} \subset \mathbb{W}_{h_k}$, **Biquadratic interpolation for the prolongation and natural embedding for the restriction.** For any $\tilde{\mathbf{u}}_{k-1} \in \mathbb{W}_{h_{k-1}}$

$$\tilde{\mathbf{u}}_{k-1} = \sum_{j=1}^{\dim \mathbb{W}_{h_{k-1}}} \tilde{\mathbf{u}}_{j,k-1} \varphi_j^{k-1} = \sum_{j=1}^{\dim \mathbb{W}_{h_k}} \tilde{\mathbf{u}}_{j,k} \varphi_j^k, \quad \tilde{\mathbf{u}}_{i,k} = \sum_{j=1}^{\dim \mathbb{W}_{h_{k-1}}} \tilde{\mathbf{u}}_{j,k-1} \mathcal{N}_j^k(\varphi_i^{k-1})$$

By using the dual basis $\{\mathcal{N}_i^k, i = 1, \dots, \dim \mathbb{W}_{h_k}\}$, i.e. $\mathcal{N}_i^k(\varphi_j^k) = \delta_{ij}$

$$\mathcal{I}_{k-1,k}^{\tilde{\mathbf{u}}} \in \mathcal{W}_k \times \mathcal{W}_{k-1}, \quad [\mathcal{I}_{k-1,k}^{\tilde{\mathbf{u}}}]_{ij} = \mathcal{N}_j^k(\varphi_i^{k-1}) \quad \mathcal{I}_{k,k-1}^{\tilde{\mathbf{u}}} = \mathbf{M}_{k-1}^{-1} \left(\mathcal{I}_{k-1,k}^{\tilde{\mathbf{u}}} \right)^T \mathbf{M}_k$$

Coarse grid operator

$$\mathcal{R}_{k-1} = \left(\mathcal{I}_{k-1,k}^{\tilde{\mathbf{u}}} \right)^T \mathcal{R}_k \quad \mathcal{J}_{k-1}^{\tilde{\mathbf{u}}} = \left(\mathcal{I}_{k-1,k}^{\tilde{\mathbf{u}}} \right)^T \mathcal{J}_k^{\tilde{\mathbf{u}}} \mathcal{I}_{k,k-1}^{\tilde{\mathbf{u}}}$$

Galerkin orthogonality is preserved and the optimal order of convergence of MG is maintained !



- Pressure, P_1^{disc} FEM approximations: Nested discontinuous approximation, $\mathbb{Q}_{h_{k-1}} \subset \mathbb{Q}_{h_k}$

The prolongation operator for pressure $\mathcal{I}_{k-1,k}^p : \mathbb{Q}_{h_{k-1}} \longrightarrow \mathbb{Q}_{h_k}$ is defined in terms of local L^2 inner-product projection operator

$$q \in P_1^{\text{disc}}(K) \implies q \in P_1^{\text{disc}}(\sigma_l(K)), l = 1, \dots, 2^d$$

$$\sum_{l=1}^{2^d} \int_{\sigma_l(K)} \mathcal{I}_{k-1,k}^p p_{k-1} q \, d\Omega = \int_K p_{k-1} q \, d\Omega, \quad \forall K \in \mathcal{T}_{h_{k-1}}$$

Its matrix representation is as follows:

$$\mathcal{I}_{k-1,k}^p = \mathbf{M}_k^{-1} \mathbf{M}_{k-1}$$

The restriction operator for pressure $\mathcal{I}_{k,k-1}^p : \mathbb{Q}_{h_k} \longrightarrow \mathbb{Q}_{h_{k-1}}$ is the transpose counterpart of the prolongation w.r.t. L^2 :

$$\forall K \in \mathcal{T}_{h_{k-1}}, q \in P_1^{\text{disc}}(K) ; \int_K \mathcal{I}_{k,k-1}^p p_k q \, d\Omega = \sum_{l=1}^{2^d} \int_{\sigma_l(K)} p_k \mathcal{I}_{k-1,k}^p q \, d\Omega$$

Its matrix representation

$$\mathcal{I}_{k,k-1}^p = \mathbf{M}_{k-1}^{-1} \mathbf{M}_k$$

Indeed the transpose of prolongation operator is the restriction operator

$$\mathcal{I}_{k,k-1}^p = (\mathcal{I}_{k-1,k}^p)^T$$



- Setting local subproblem,

- Prolongation/Restriction: $\mathcal{P}_K = (\mathcal{P}_K^{\tilde{u}}, \mathcal{P}_K^p)$, $\mathcal{P}_K^T = (\mathcal{P}_K^{\tilde{u}^T}, \mathcal{P}_K^{p^T})$

$$\mathcal{P}_K^{\tilde{u}} : \mathbb{W}_h(K) \longrightarrow \mathbb{W}_h, \quad \mathcal{P}_K^p : \mathbb{Q}_h(K) \longrightarrow \mathbb{Q}_h, \quad \forall K \in \mathcal{T}_h,$$

$$\mathcal{P}_K^{\tilde{u}^T} : \mathbb{W}_h \longrightarrow \mathbb{W}_h(K), \quad \mathcal{P}_K^{p^T} : \mathbb{Q}_h \longrightarrow \mathbb{Q}_h(K), \quad \forall K \in \mathcal{T}_h,$$

- Algebraically counterpart

- Prolongation/Restriction: $\mathcal{P}_K = (\mathcal{P}_K^{\tilde{u}}, \mathcal{P}_K^p)$, $\mathcal{P}_K^T = (\mathcal{P}_K^{\tilde{u}^T}, \mathcal{P}_K^{p^T})$

$$\mathcal{U}_K = (\tilde{u}_K, p_K) := \mathcal{P}_K^T \mathcal{U} = (\mathcal{P}_K^{\tilde{u}^T} \tilde{u}, \mathcal{P}_K^{p^T} p)$$

$$\mathcal{U} = (\tilde{u}, p) := \sum_{K \in \mathcal{T}_h} \mathcal{P}_K \mathcal{U}_K = \sum_{K \in \mathcal{T}_h} (\mathcal{P}_K^{\tilde{u}} \tilde{u}, \mathcal{P}_K^p p)$$

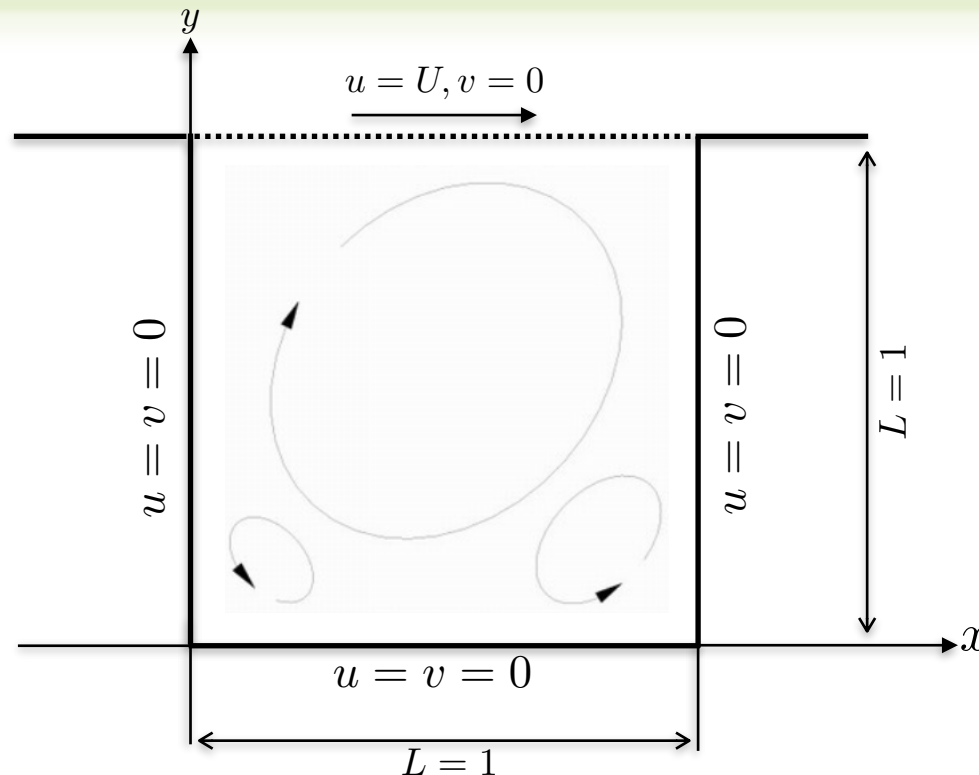
- Block Gauss-Seidel iteration reads

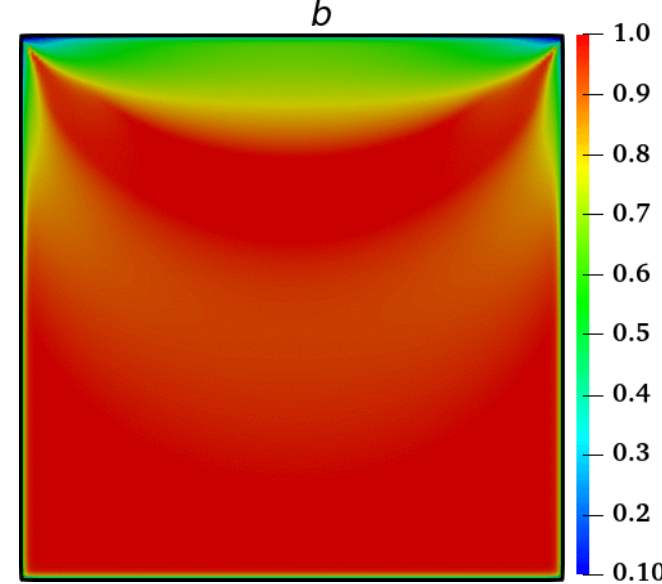
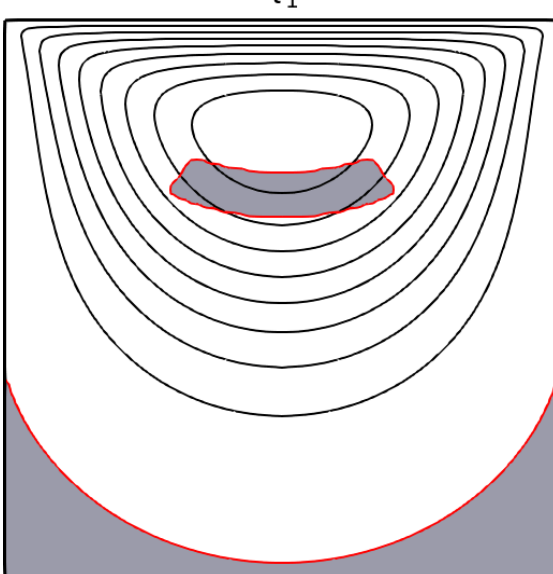
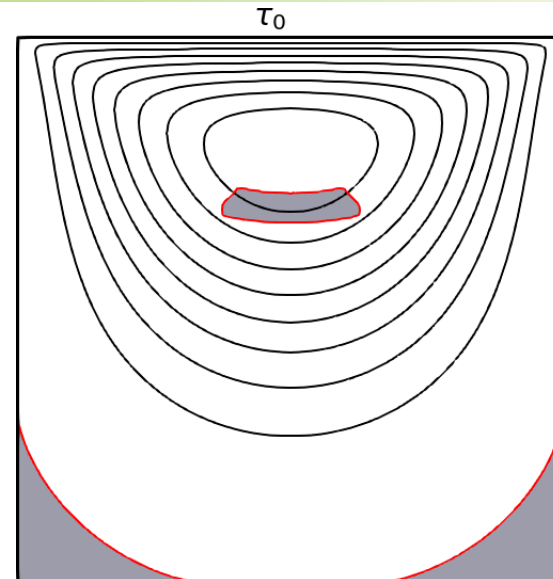
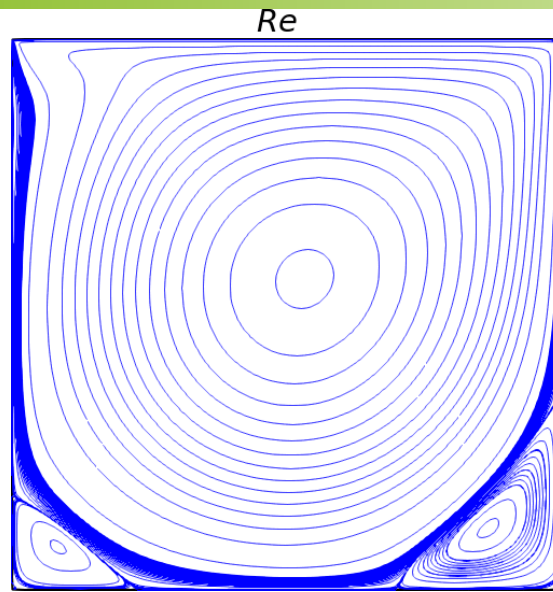
$$\mathcal{U}^{k+1} = \mathcal{U}^k - \omega_k \sum_{K \in \mathcal{T}_h} \mathcal{P}_K \left(\mathcal{P}_K^T \left(\frac{\partial \mathcal{R}(\mathcal{U}^k)}{\partial \mathcal{U}} \right) \mathcal{P}_K \right)^{-1} \mathcal{P}_K^T \mathcal{R}(\mathcal{U}^k).$$

Coupled Monolithic Multigrid Solver !

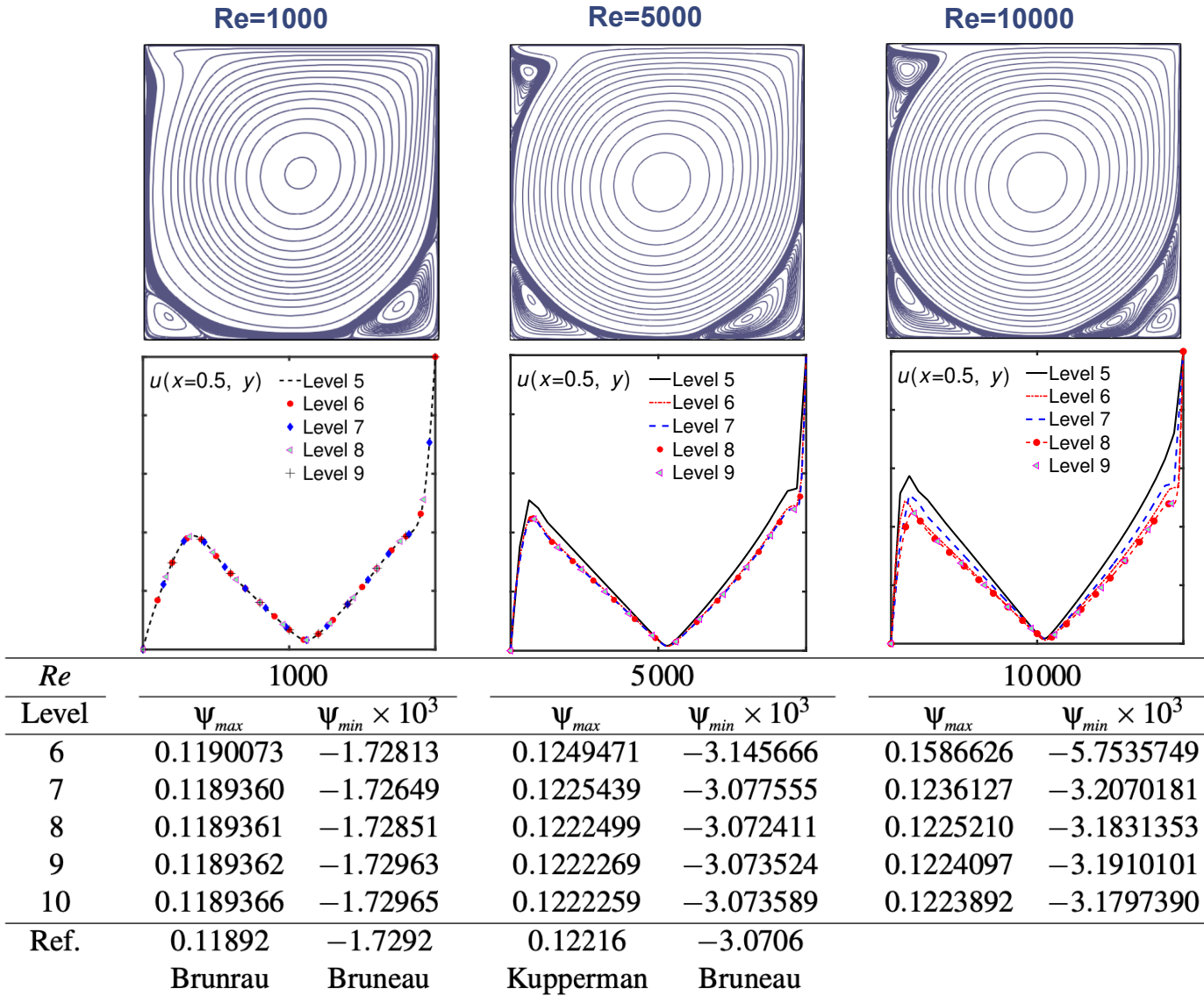


- Starting point: consider flow in a cavity with unit height
- Steady, incompressible flow
- Constant speed at upper lid
- No-slip Dirichlet boundary conditions





- Point-wise convergence for Newtonian flow



- **Global quantity and solver behaviour**

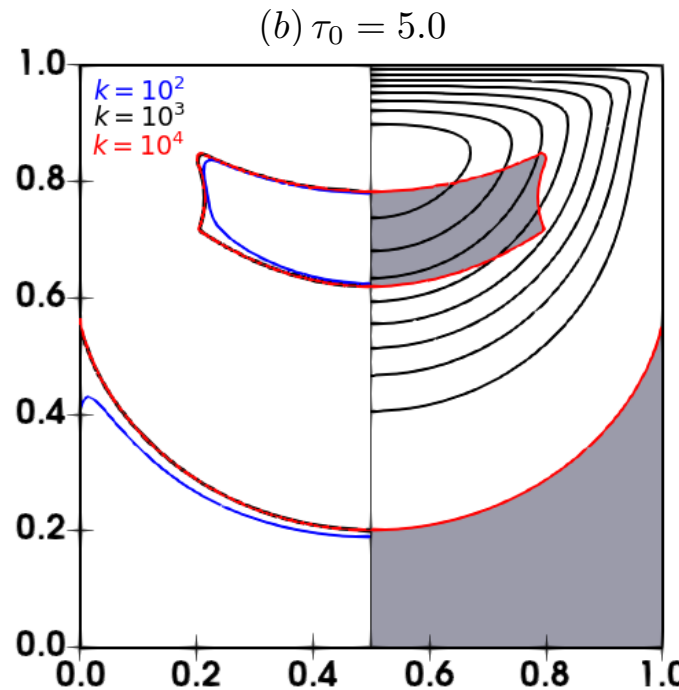
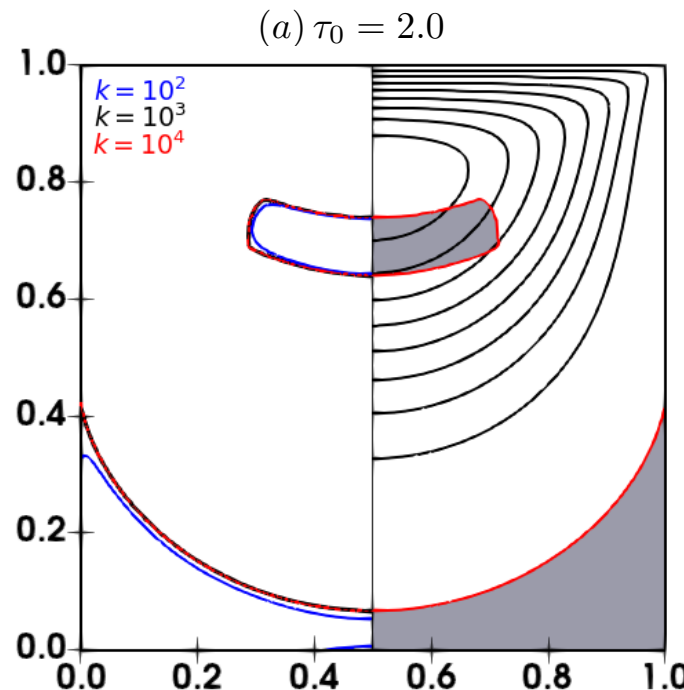
<i>Re</i>	1000		5000		10000	
	Level	cells	Energy $\times 10^2$	N/M	Energy $\times 10^2$	N/M
5	1024	4.541506	5/1	6.082524	6/1	7.940472
6	4096	4.458877	5/1	4.955858	5/1	5.369527
7	16384	4.452357	3/1	4.768669	4/1	4.868399
8	65536	4.451904	3/1	4.744815	3/2	4.783917
9	262144	4.451846	3/1	4.742921	3/1	4.773500
10	1048576	4.451834	2/1	4.742815	3/1	4.772692
<i>Ref. values</i> \approx :		4.45		4.74		4.77

- ✓ Mesh convergence of the solutions irrespective of Re number
- ✓ Efficient non-linear solver
- ✓ Mesh independent linear solver

Accurate, robust and efficient Monolithic Multigrid Solver



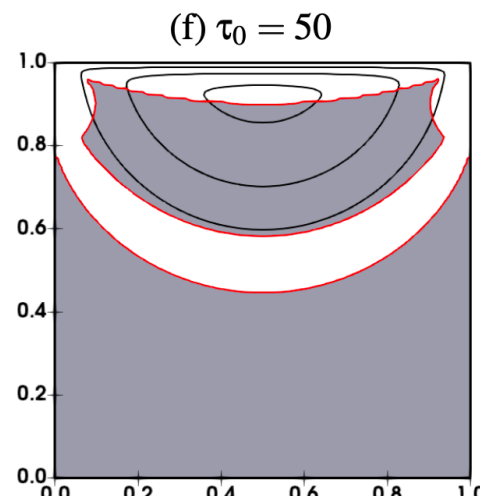
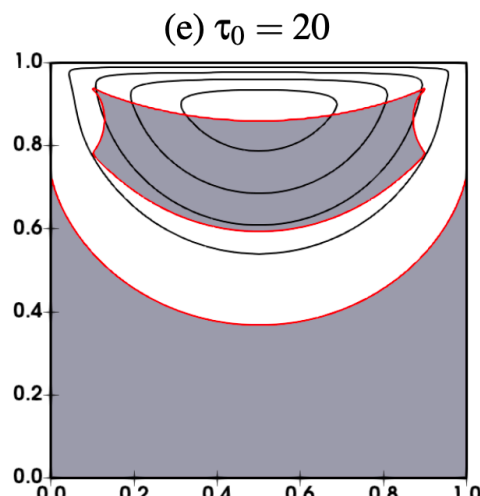
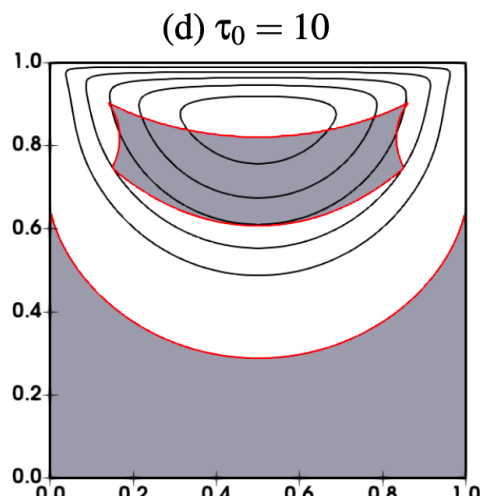
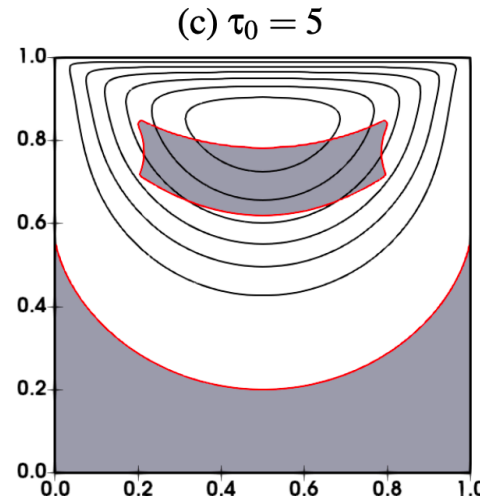
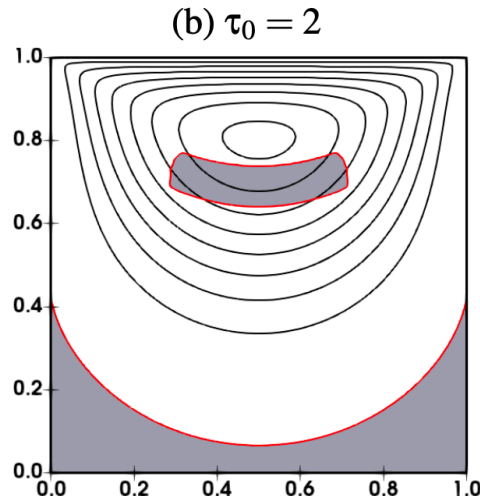
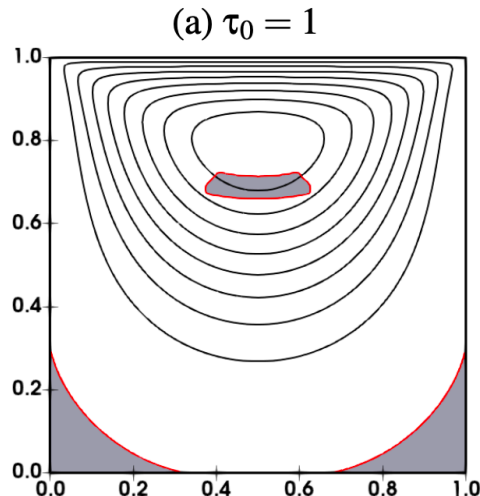
- Boundary limit for rigid-zone w.r.t regularization k



- Accurate track of interface requires
 - ✓ larger k solutions
 - ✓ finer mesh refinement
- Existence of pair (k, L) beyond which no further improvement in solutions is expected

Viscoplastic flow in Lid-driven cavity

- progressive growth of unyielded zones for non-thixotropic (Bingham Plastic) flow



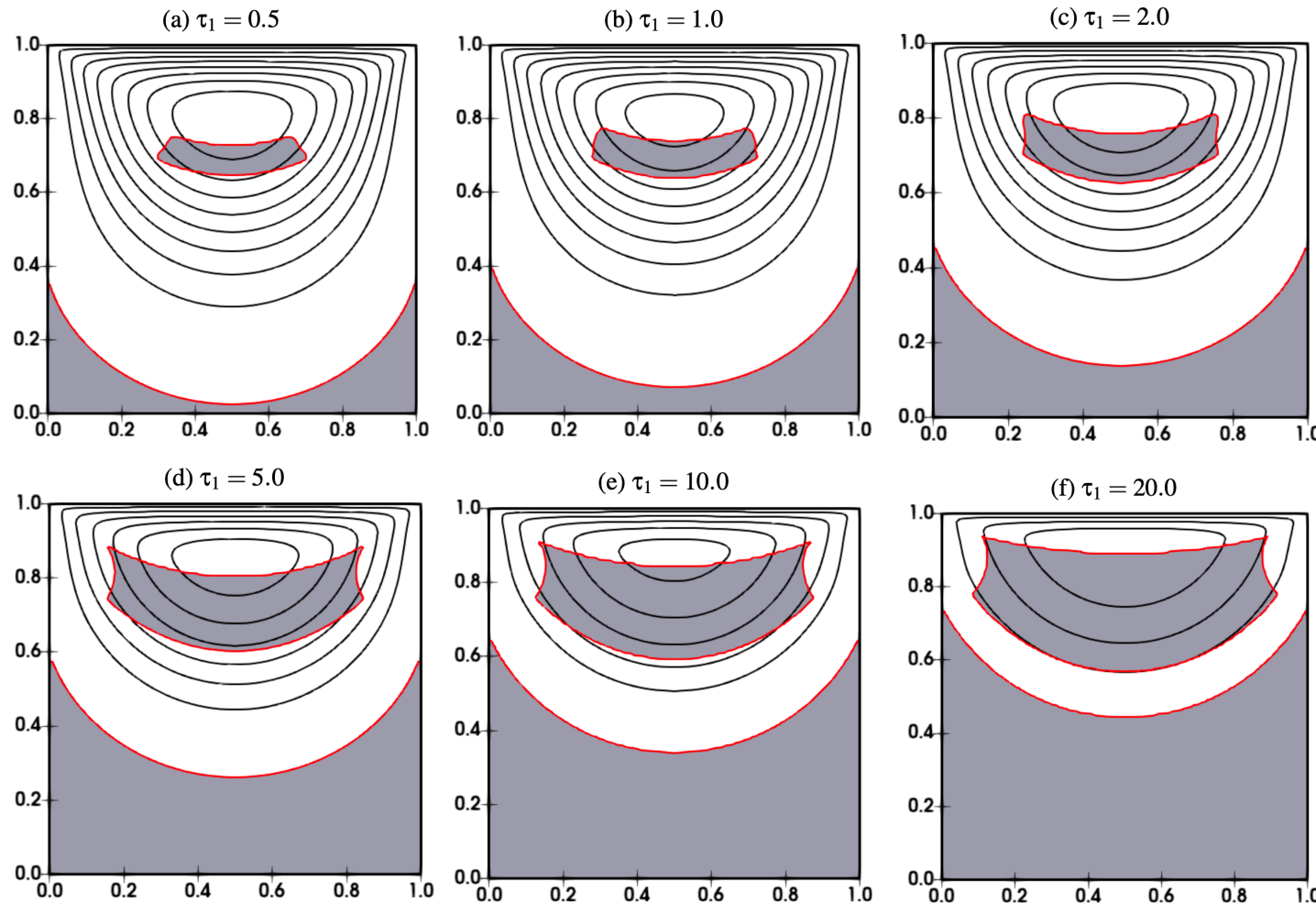
✓ Unyielded zones's shape and extent is in agreement with Ref. Results

- Solver behaviour w.r.t Regularization and mesh refinement

$k \backslash L$	5	6	7	5	6	7	5	6	7
$\tau_0 = 1.0$									
1×10^1	3/1	3/1	3/1	3/1	3/1	3/1	4/1	4/1	4/1
5×10^1	2/1	2/1	2/1	2/1	2/1	2/1	3/1	3/1	3/1
1×10^2	3/1	3/1	3/1	3/1	3/1	3/1	4/1	4/1	4/1
5×10^2	3/1	2/1	2/1	3/1	2/1	3/1	3/2	3/2	3/1
1×10^3	2/2	3/2	3/1	3/1	3/1	4/1	4/1	5/2	5/2
5×10^3	2/1	2/1	4/1	3/1	3/2	6/2	4/1	8/2	6/1
1×10^4	2/1	2/2	5/1	3/1	3/1	6/1	4/1	5/4	6/3
$\tau_0 = 10.0$									
1×10^1	5/1	5/1	5/1	6/1	6/1	6/1	5/1	7/1	7/1
5×10^1	4/1	3/1	3/1	4/1	4/1	3/2	5/4	4/2	4/2
1×10^2	5/2	4/1	4/1	5/2	5/2	5/1	6/5	5/4	5/1
5×10^2	5/3	3/2	3/1	4/4	3/4	4/3	5/4	4/2	4/3
1×10^3	5/2	7/4	9/1	5/5	7/2	8/1	5/5	9/2	9/2
5×10^3	5/1	7/3	8/2	6/3	6/4	6/4	6/4	7/2	8/2
1×10^4	6/1	7/2	8/3	6/3	5/5	7/3	6/3	7/3	8/2

- ✓ Efficient non-linear solver
- ✓ Mesh independent linear solver
- ✓ Solutions are obtained with continuation strategy w.r.t. k
- Integration of continuation strategy w.r.t. k in the solver

- Impact of thixotropic yield stress on morphology of unyielded zones in TVP flow



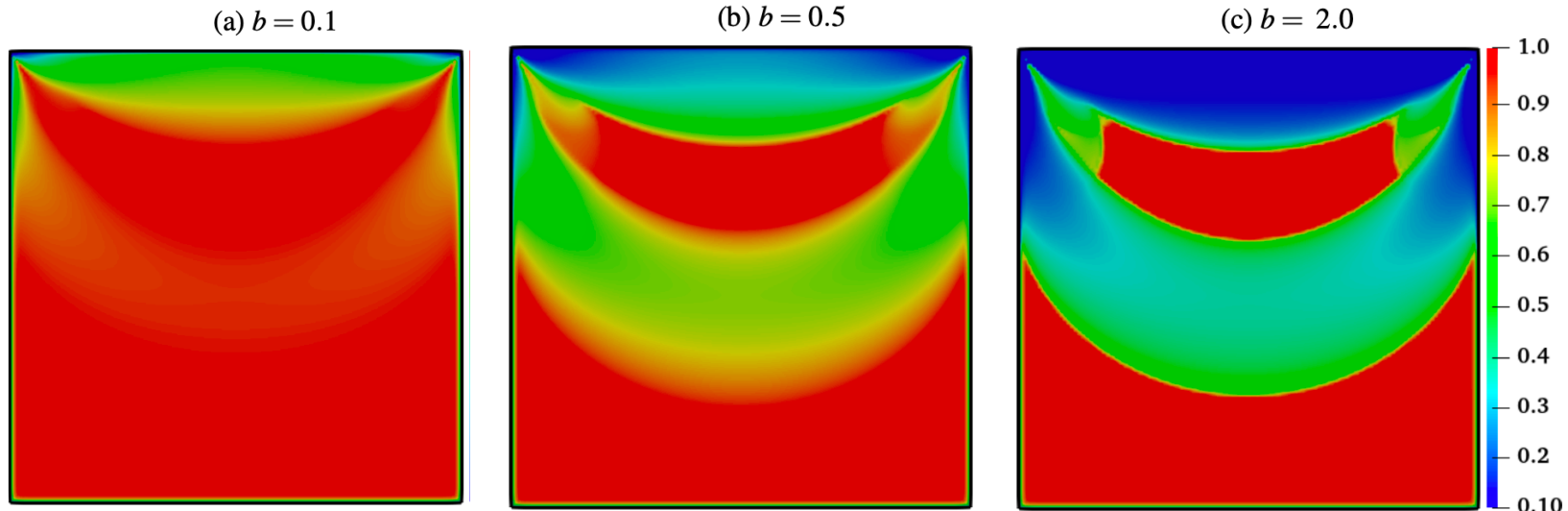
- ✓ Main rheological characteristics of materials with yield stress is preserved

- Solver behaviour w.r.t Regularization and mesh refinement

$k \setminus L$	5	6	7	5	6	7	5	6	7
	$\tau_1 = 0.5$			$\tau_1 = 1.0$			$\tau_1 = 2.0$		
1×10^1	5/2	5/3	6/2	5/2	5/2	9/1	5/2	5/2	9/1
5×10^1	4/2	4/2	4/2	3/2	3/3	7/1	3/2	3/3	8/1
1×10^2	4/1	4/2	5/1	4/1	4/2	7/1	4/2	4/2	8/1
5×10^2	4/1	4/1	5/1	3/1	4/1	6/1	4/2	4/2	8/1
1×10^3	4/1	4/1	4/1	4/2	4/2	8/1	4/4	6/1	7/1
5×10^3	4/1	4/1	3/2	7/1	9/1	5/1	6/1	9/1	8/1
1×10^4	4/1	4/2	4/2	5/1	7/1	4/1	7/1	10/1	8/2
	$\tau_1 = 5.0$			$\tau_1 = 10.0$			$\tau_1 = 20.0$		
1×10^1	6/2	6/2	10/1	11/1	8/2	11/1	10/1	9/2	11/1
5×10^1	4/2	3/2	11/1	11/1	4/2	7/1	12/1	5/3	9/1
1×10^2	4/2	5/2	11/1	10/1	5/3	8/1	12/1	6/3	10/1
5×10^2	5/2	4/2	10/1	9/1	5/3	5/1	8/1	5/5	11/1
1×10^3	5/2	9/1	10/1	10/1	9/1	7/1	8/2	9/1	9/2
5×10^3	5/1	5/1	5/1	8/1	8/2	6/1	8/1	7/1	11/1
1×10^4	5/1	5/2	5/1	8/3	7/1	5/1	8/2	7/1	9/1

- ✓ Robust non-linear solver
- ✓ Mesh independent linear solver
- ✓ Solutions are obtained via continuation strategy w.r.t. k
- ➔ Integration of continuation strategy w.r.t. k in the solver

- Material micro-structural level w.r.t. breakdown parameter



- Interplay of yield stress and thixotropy

- ✓ Structuring level is predicting shape and extent of rigid zones
- ✓ Induction of more breakdown layers
- ✓ Shear localization
- ✓ Shear band

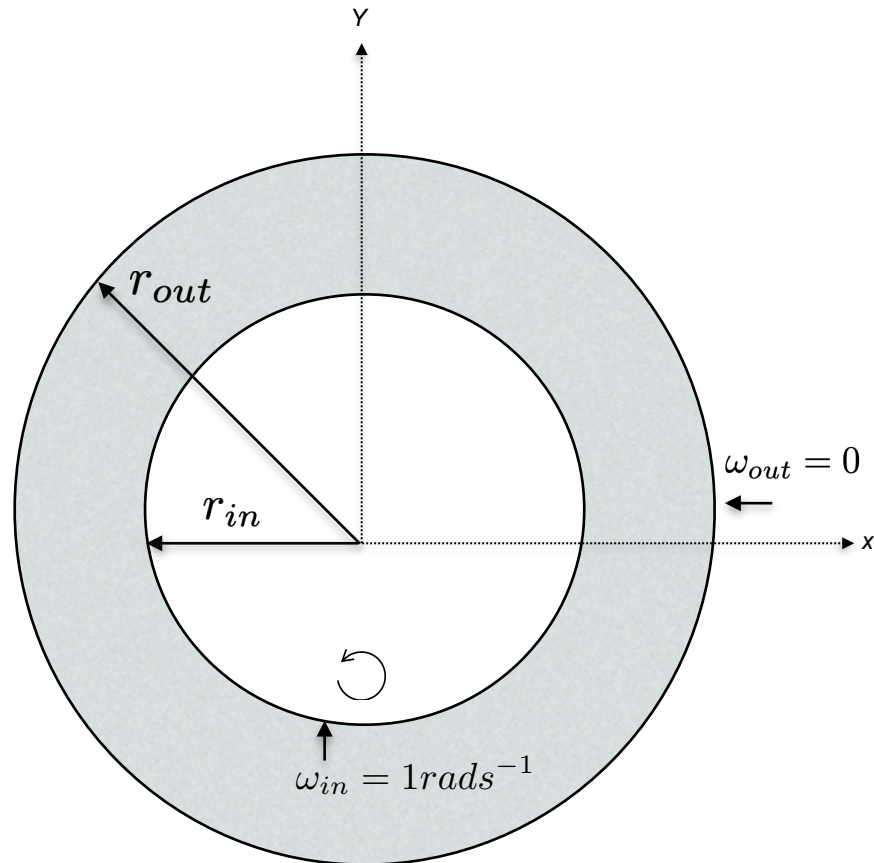
Continuous axial-Flow Couette device:

The material is sheared in the annulus between the interior and exterior cylinder shells of radii r_{in} and r_{out} respectively.

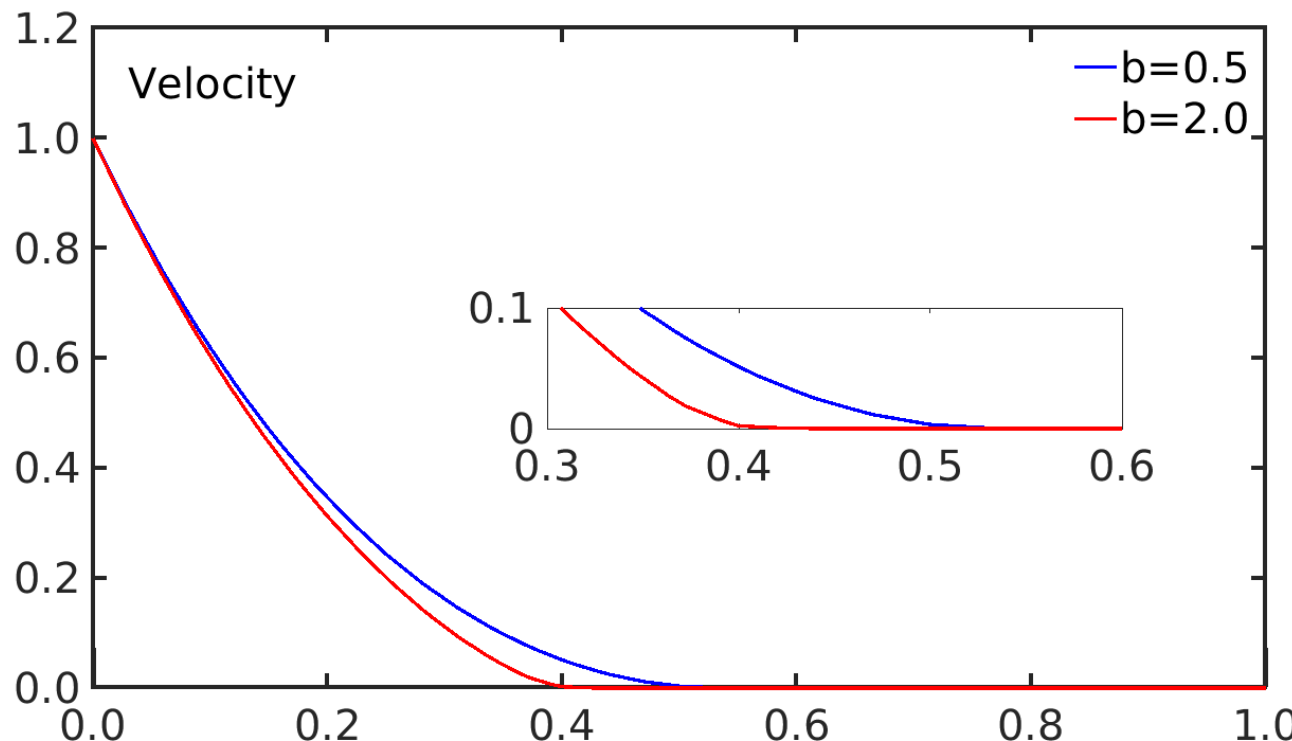
- ▶ Concentric cylinders
- ▶ Rotating inner cylinder with $\omega_{in} = 1 \text{ rads}^{-1}$
- ▶ Stationary outer cylinder
- ▶ Vertical flow super-imposed in radial direction

Investigations of thixo-viscoplastic phenomena

- ▶ Shear localization
- ▶ Shear banding
- ▶ Consistent transition points between velocity and structure
- ▶ Discontinuous jump to infinity for viscosity

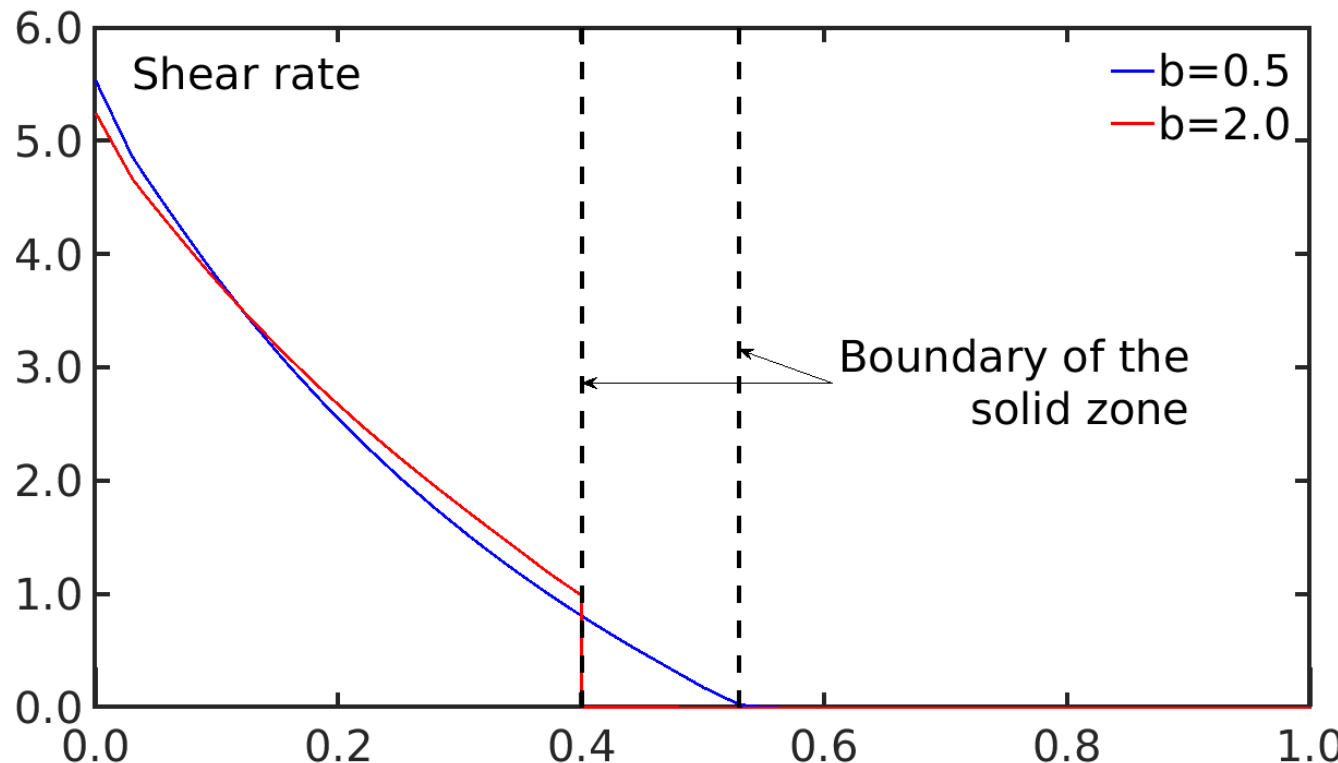


- Velocity profile at cut-line positions $c; c \in [0, 2\pi]$ in a Couette device w.r.t breakdown parameter



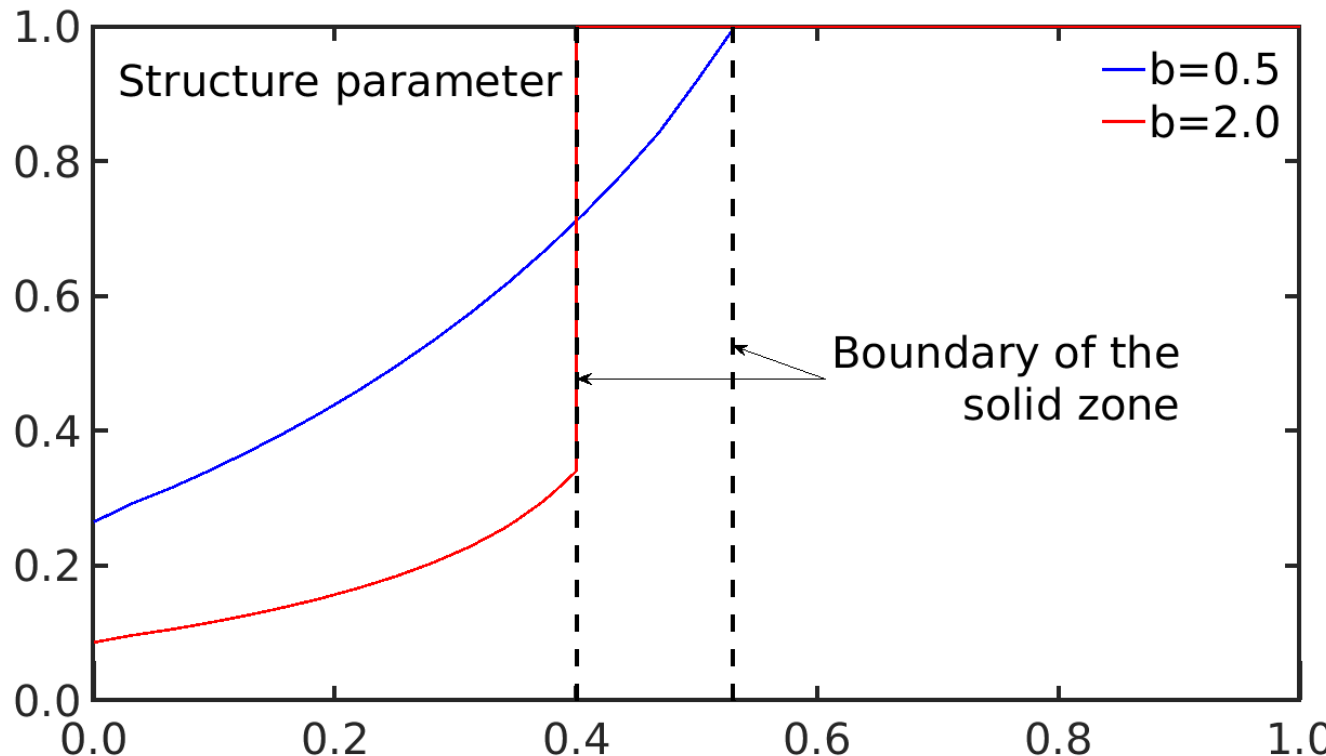
- ✓ Localization
- ✓ Shear banding

- Shear rate at cut-line positions $c; c \in [0, 2\pi]$ in a Couette device w.r.t breakdown parameter



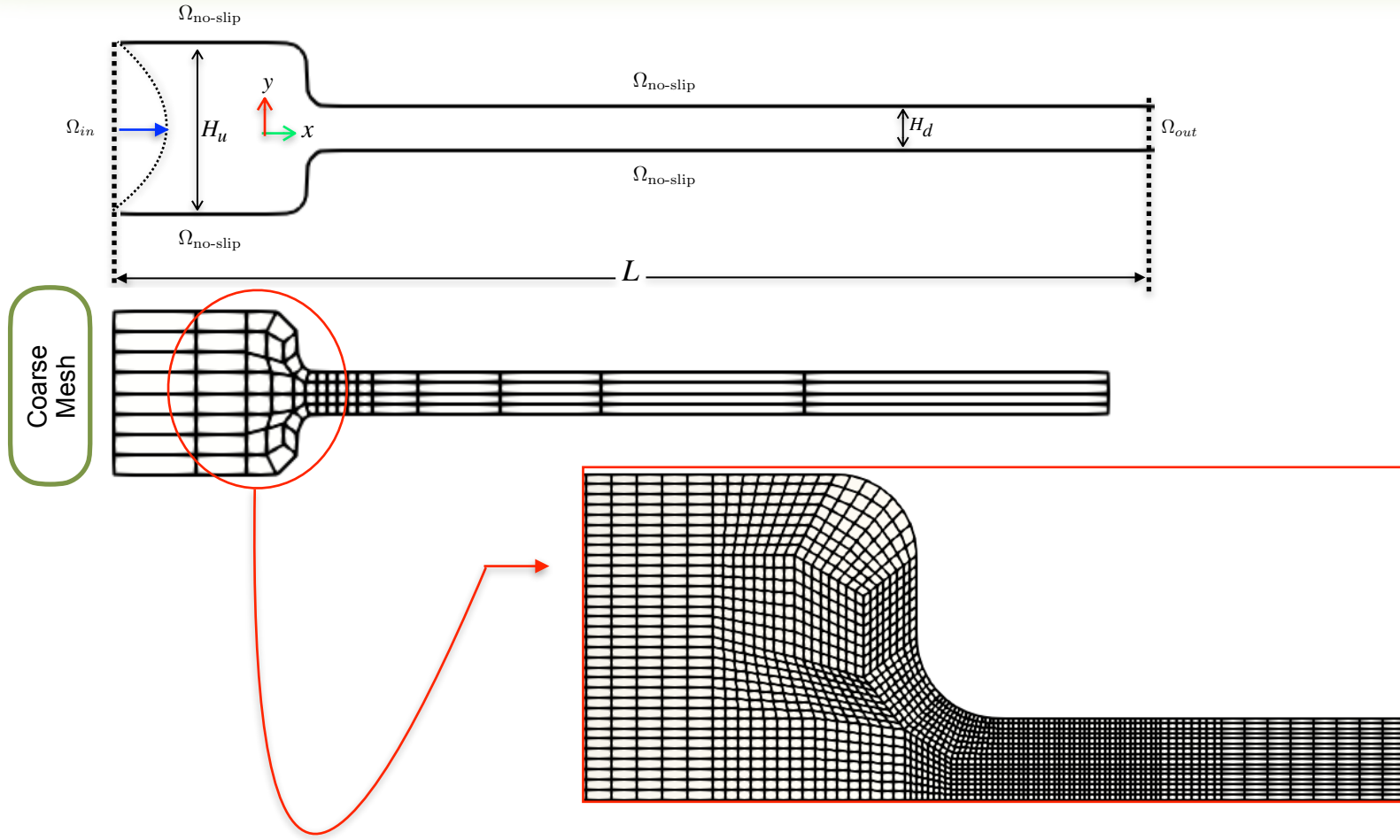
- ✓ Smooth and sharp transition are possible
- ✓ Transition point matches with the velocity

- Structure parameter at cut-line positions $c; c \in [0, 2\pi]$ in a couette w.r.t. breakdown parameter

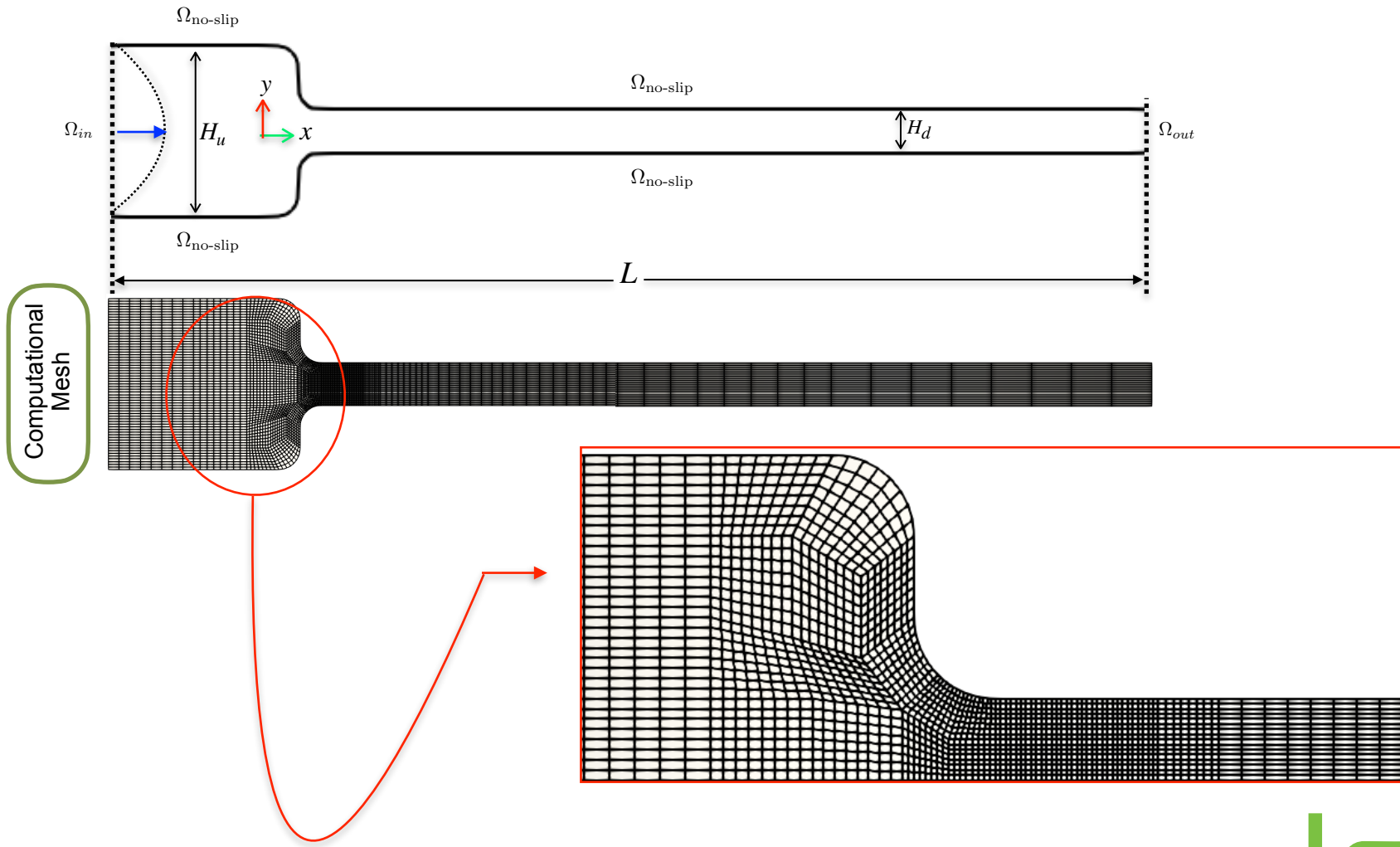


- ✓ Transition point matches with the velocity
- ✓ Structuring level is predicting shape and extent of rigid zones

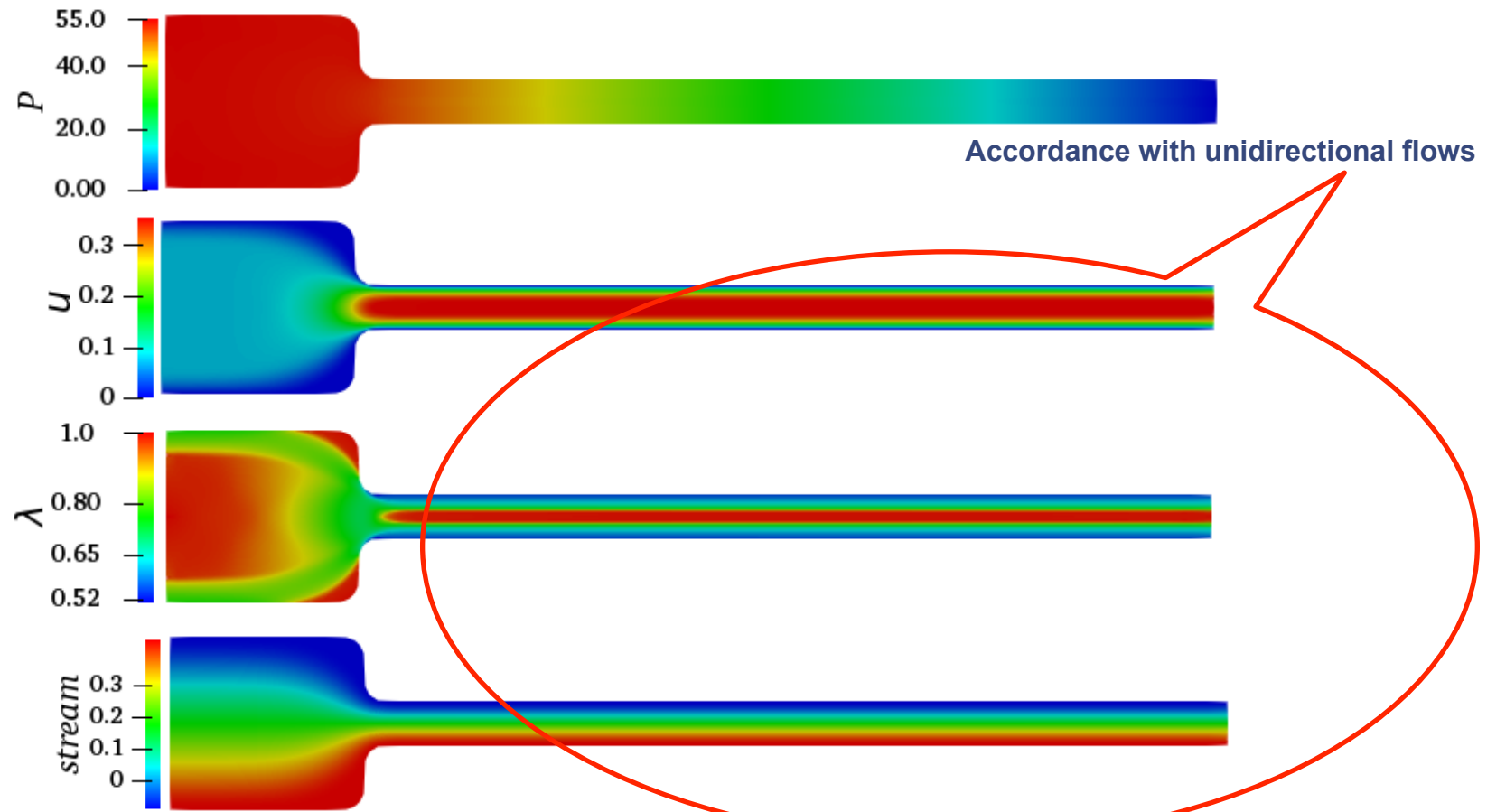
- 2D-FEM simulation results for thixo-viscoplastic flow- validation of 1D tool
- Specifying the “unidirectional profiles as boundary Data” in 2D for contraction



- 2D-FEM simulation results for thixotropic flow- validation of 1D tool
- Specifying the “1D-profiles as boundary Data” in 2D simulations for contraction domain



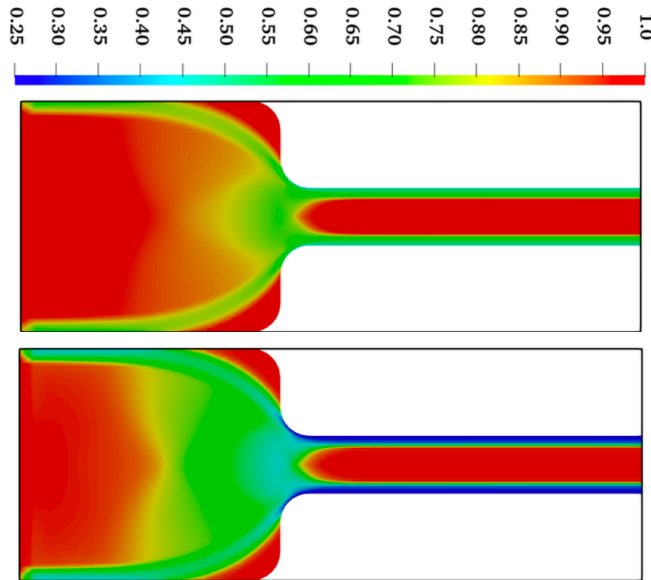
Contraction flow (smoothed)



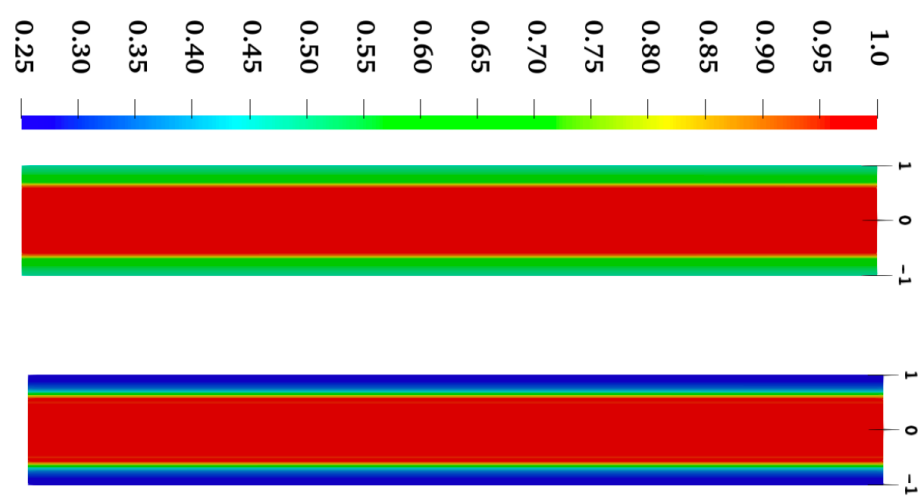
- ✓ As predicted (u, λ, p) solutions
- ✓ Structuring level is predicting shape and extent of rigid zones

- Material micro-structural level w.r.t. breakdown

(i) Upstream channel & Entrance zone



(ii) Downstream channel



- Inherent thixotropy speed-up the breakdown

- ✓ Appearance of more breakdown layers
- ✓ Applications: restart pressure in pipelines should not be over-estimated

We analysed FEM for regularized TVP problem

- ✓ Wellposedness
- ✓ Convergence analysis

Analyzed the accuracy, robustness, and efficiency of the TVP solver using

- ✓ Higher order finite element method
- ✓ Monolithic Newton-multigrid
 - Adaptive discrete Newton's method with global convergent property
 - Geometric multigrid with local MPSC

Simulations for TVP materials for Benchmarks in Lid-driven cavity, Couette devices and 4:1 contraction configuration



FEM analysis and monolithic Newton-multigrid solver for thixo-viscoplastic flow problems

N. Begum, A. Ouazzi, S. Turek
Institute of Applied Mathematics, LS III,
TU Dortmund University, Dortmund, Germany

8th European Congress on Computational Methods in Applied Sciences and Engineering
ECCOMAS Congress 2022
5-9 June 2022, Oslo, Norway